

Degenerate bound states in the continuum in square and triangular open acoustic resonators

Almas Sadreev,^{1,*} Evgeny Bulgakov,¹ Artem Pilipchuk,¹ Andrey Miroshnichenko,² and Lujun Huang²

¹*Kirensky Institute of Physics Federal Research Center KSC SB RAS 660036 Krasnoyarsk Russia*

²*School of Engineering and Information Technology,
University of New South Wales Canberra, Northcott Drive, AC, 2600, Australia*

We consider square and equilateral triangular open acoustic resonators with the C_{4v} and C_{3v} symmetries, respectively. There is a unique property of square and triangular resonators of accidental number four-fold degeneracy of eigenstates that gives rise to two-fold degenerate Friedrich-Wintgen (FW) BICs. Compared to usual FW BICs the degenerate FW BICs maintain high Q -factor in wide range of the size of resonators. That removes the fabrication difficulties of proper choice of resonator. The presence of degenerate BICs in triangular resonators is extremely sensitive to switch output flows by small perturbations with 100% efficiency.

I. INTRODUCTION

A new paradigm for trapping and confining of the resonant modes have emerged in recent years based on the bound states in the continuum (BICs) in wave systems. BICs, also known as trapping mode with infinite large Q -factor, have triggered extensive interest in photonic and acoustic communities [1–5]. The most straightforward mechanism of BICs is the symmetrical incompatibility of closed system states with propagating states of the continuum [6–10]. More interesting, Friedrich-Wintgen (FW) BICs are result of full destructive interference of two or more resonant modes competing for leakage into open channels of waveguides [4, 11, 12]. The FW BICs can be realized in open resonators by gradual change of aspect ratio of the resonator when a degeneracy of eigenfrequencies occur [12]. In acoustic systems, the FW BICs were considered by many scholars [13–17]. The experimental evidence for the FW BICs was reported by Lepetit and Kanté [18] and by Huang *et al* [19] in the most straightforward configuration of rectangular resonator opened to attached waveguide.

Although the last time BICs have been successfully demonstrated in different acoustic resonators fabricated by 3D printing, the Q -factor of quasi-BICs is sensitive to the structure imperfections. Moreover continual variation of aspect ratio of the resonator for achievement FW BICs is very challenging for any type of resonator, acoustic, metallic or dielectric. Therefore, a search of FW BICs not sensitive to the aspect ratio of resonators is highly desired. In the present paper, we advocate square or equilateral triangular resonators with the group symmetries C_{4v} and C_{3v} , respectively. Its eigenmodes ψ_{mn} and eigenfrequencies ν_{mn}^2 exhibit trivial degeneracy by permutation of indices $m \leftrightarrow n$. Here the eigenfrequencies are given in terms of the frequency $\omega_0 = \pi s/a$, where s is the velocity of sound or light in air, and a is the side size of the resonator. Therefore, one can expect that opening of the resonator by attachment of waveguides transforms these degenerate eigenmodes into superradiant mode and FW BIC for granting as it follows from the FW mechanism of BICs which occur at degeneracy of eigenfrequencies [4, 11, 12, 20]. Variants of attachment of waveguides to a square resonator are sketched in Fig. 1. However, for the case (a) in Fig. 1 the FW BICs occur only after deformation of square resonator into the rectangular one [19]. The reason for cancellation of FW BICs is lowering of the symmetry C_{4v} of closed square resonator towards C_{2v} after the (a) case opening. Quantitatively, the coupling of eigenmodes of a square resonator with evanescent modes of waveguides perturbs the eigenfrequencies of the resonator and removes the permutation degeneracy of open square resonator [21]. Next, consider the cases in which for opening of the resonators the symmetry C_{4v} is preserved as sketched in Fig. 1 (b) and (c). In this case the degenerate eigenmodes (m, n) and (n, m) of closed resonator and their resonant counterparts of open resonator both are classified according to the different irreducible representations of the group C_{4v} and therefore can not be coupled via the continuum of waveguides that cancels the FW mechanism of the BICs too. The same consideration is applied to equilateral triangular resonator with the symmetry group C_{3v} .

However, there is a unique case of accidental or number degeneracy of eigenmodes over two-fold in the square and equilateral triangle $\nu_{mn}^2 = \nu_{m'n'}^2$. For example, in square acoustic resonator two choices of integers $m = 1, n = 6$ and $m' = 5, n' = 4$ have the same frequency $25/a^2$ [22, 23]. That brings four-fold degeneracy of a closed resonator that plays the key role in the existence of two-fold degeneracy of the FW BICs provided that open resonators preserve the group symmetries C_{4v} or C_{3v} as shown in Fig. 1 (b)-(d). We show that the degenerate FW BICs are classified

* Corresponding Author; almas@tnp.krasn.ru

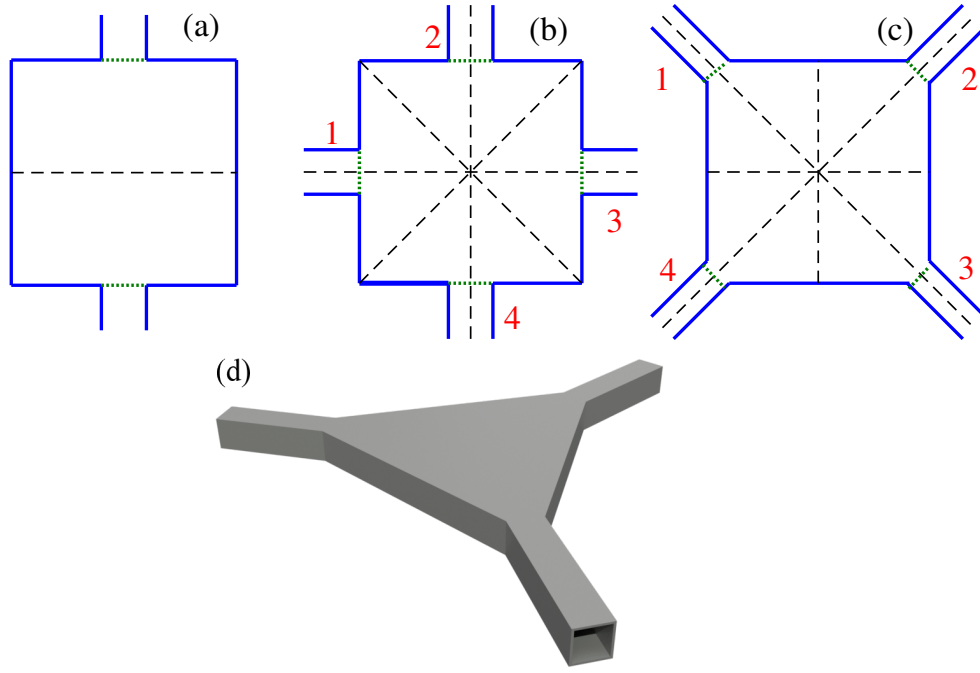


Figure 1. (a) Two waveguides attached to square resonator with the symmetry C_{4v} lower the symmetry of open system till inversion symmetry σ , (b) and (c) Four identical waveguides attached to square resonator preserve the symmetry C_{4v} . (d) three waveguides attached to equilateral triangle resonator preserve the symmetry C_{3v} .

according to the two-dimensional irreducible representation E of these group symmetries. Without loss of generality we focus on the acoustic resonators with Neumann boundary conditions in which BICs can be directly probed by microphone measurements of acoustic pressure inside resonators [17, 19]. Actually, resonators are three-dimensional, but the acoustic resonators allow completely disregard the third dimension if the thickness of the resonator is small enough compared to longitudinal sizes as sketched in Fig. 1 (d). In that case, the solutions are constant over the third dimension to be excluded from the solutions presented in Appendix. That opens many ways for experimental verifications of theoretical predictions outlined below in the square and equilateral triangle resonators.

II. THE SP BICS DUE TO PERMUTATION SYMMETRY IN OPEN SQUARE RESONATOR

The symmetry of the open resonators is important for classification and establishment of BICs. For dielectric resonators embedded into radiation space the total symmetry is given by the structure that determines multipole classification of radiation and the symmetry of ultra-high Q resonances (quasi-BICs) of the structure consisted of one or a few symmetrical dielectric cavities [24–26]. The symmetry of BICs in photonic crystals is given by the symmetry of the crystals [27–30]. As different from the above, the symmetry of resonators with attached directional waveguides is determined by compatibility of symmetry of closed resonator with the symmetry of waveguides. The symmetry of the total system can be lowered or coincide with the symmetry of closed resonator as illustrated in Fig. 1.

The eigenmodes and eigenfrequencies of the acoustic square resonator are collected in Appendix. There are two distinct pairs of degenerate states $\psi_{m,n}, \psi_{n,m}, m \neq n$. The first pair of the eigenmodes with $m - n$ odd is classified according to the two-dimensional irreducible representation E . The particular case of $m = 2, n = 3$ is demonstrated in Fig. 6 of Appendix. The second pair with $m - n$ even is classified according to the reducible representations. Only the linear combinations $\psi_{m,n} \pm \psi_{n,m}$ are classified according to the irreducible one-dimensional representations B_1 and A_1 or B_2 and A_2 respectively. A particular case of eigenmodes ψ_{24} and ψ_{42} classified according to B_2 and A_2 is shown in Fig. 7 in Appendix.

Opening of the resonator transforms the real eigenfrequencies of the closed resonator into the complex eigenfrequencies. The procedure of transition from closed system onto open system can be performed by use of the Feshbach projection technique that results in the non Hermitian effective Hamiltonian [31–36]. The complex eigenvalues of this Hamiltonian respond for the position of resonances and resonant line widths and therefore provide excellent way to establish BICs as eigenmodes of effective Hamiltonian with real eigenvalues [4]. The specific form of the effective non

Hermitian Hamiltonian is given in Appendix applied to open acoustic resonators [36].

Let us first consider the degenerated pair of eigenmodes of closed square resonator $\psi_{m,n}, \psi_{n,m}$ with $m - n$ odd and $m \neq n$ classified according to the two-dimensional representation E , for example, the pair presented in Appendix ψ_{23} and ψ_{32} . The coupling matrix elements of these modes with the first open channel $p = 1$ and the second closed channel $p = 2$ for the case in Fig. 1 (b) are collected in Appendix. As a result, we can write the effective non-Hermitian Hamiltonian projected into these modes whose general form is given in Eq. (10) of Appendix

$$\hat{H}_{eff} = \begin{pmatrix} 5/a^2 - 2ik_1|k_2|\alpha^2 + 2|k_2|\beta^2 & 0 \\ 0 & 5/a^2 - 2ik_1|k_2|\alpha^2 + 2|k_2|\beta^2 \end{pmatrix}. \quad (1)$$

Here according to Table 2 of Appendix we introduced the notations $\alpha = W_{2,3;p=1,C=1} = -\frac{2}{\pi} \sin \frac{\pi}{a}$, $\beta = W_{2,3;p=2,C=1} = f(a)$. The case of Fig. 1 (c) gives the similar diagonal matrix

$$\hat{H}_{eff} = \begin{pmatrix} 5/a^2 - 4ik_1|k_2|\gamma^2 + 4|k_2|\delta^2 & 0 \\ 0 & 5/a^2 - 4ik_1|k_2|\gamma^2 + 4|k_2|\delta^2 \end{pmatrix}. \quad (2)$$

Here the coupling strengths γ and δ can be evaluated only numerically by integration over thin dotted lines shown in Fig. 1 (c). Irrespectively we obtain that the degenerate pair of eigenmodes $\psi_{2m,2n+1}$ and $\psi_{2n+1,2m}$ transforms into two degenerate resonances but not BICs. That has clear physical origin. Since the symmetry of the open resonator C_{4v} is preserved the eigenmodes of the closed resonator $\psi_{2,3}$ and $\psi_{3,2}$ are modified but can not be coupled through the open continuum $p = 1$ of waveguides owing to the symmetry C_{4v} of the open square resonator. As a result the FW mechanism of BICs is cancelling.

Next, we consider the pair $\psi_{s,a} = \psi_{m,n} \pm \psi_{n,m}$, $m \neq n$ and $m - n$ even which are classified according to the one-dimensional irreducible representations B_2 and A_2 . Example of these eigenfunctions $m = 2, n = 4$ are illustrated in Fig. 7 of SI. For the case in Fig. 1 (b) all coupling matrix elements with the first open channel of each waveguide equal zero as clearly seen in 7 of SI. As a result only closed channels of waveguides contribute in the effective Hamiltonian which in the space of the eigenmodes $\psi_{2,4}$ and $\psi_{4,2}$ takes the following form

$$\hat{H}_{eff} = \begin{pmatrix} 10/a^2 + 4|k_2|(b(a)^2 + c(a)^2) & -4|k_2|b(a)c(a) \\ -4|k_2|b(a)c(a) & 10/a^2 + 4|k_2|(b(a) + c(a)^2) \end{pmatrix}. \quad (3)$$

Therefore we have two SP BICs $\psi_{s,a}$ shown in Fig. 2 of SI with the eigenfrequencies

$$\nu_{s,a}^2 = 10/a^2 + 4|k_2| \begin{cases} b(a)^2 \\ c(a)^2 \end{cases} \quad (4)$$

where the coupling constants $b(a), c(a)$ are collected in Eq. (16) of SI.

III. THE TWO-FOLD DEGENERATE BICS IN OPEN SQUARE RESONATOR

As it was said in the Introduction there is the accidental number degeneracy of two doublets each degenerated by permutation of indices. For example, eigenmodes with indices 1,6 and 4,5, both classified according to the two-dimensional irreducible representation E have the same eigenvalue $\nu_{16}^2 = \nu_{4,5}^2 = 25/a^2$. The next quartet of degenerated eigenmodes is, for example, 3,10, 10,3 and 7,8, 8,7 with the eigenvalue $85/a^2$. It is reasonable to project the effective non-Hermitian Hamiltonian onto this space of the eigenmodes. Let us enumerate the eigenmodes as follows

$$\phi_1 = \psi_{1,6}, \phi_2 = \psi_{5,4}, \phi_3 = \psi_{6,1}, \phi_4 = \psi_{4,5}.$$

In order to close the second channel $p = 2$ of waveguides, we consider the eigenfrequencies of the resonator below the second cutoff of the waveguide, i.e., $\nu_{m,n}/a < 1$ if to express side sizes of resonators a via the width of waveguides $d = 1$. In particular, for the eigenstates under consideration the size of resonator is to exceed $a > 5$.

Let us, first, consider the case of sidewall connection of waveguides as shown in Fig. 1 (b). The coupling matrix elements of these eigenmodes with open channel $p = 1$ and closed channel $p = 2$ are collected in Tables II and III of Appendix. As a result, we obtain for the effective Hamiltonian in truncated Hilbert space of the eigenfunctions

$\phi_j, j = 1, 2, 3, 4$

$$\hat{H}_{eff} = \frac{1}{a^2} \begin{pmatrix} \hat{h}_{eff} & 0 \\ 0 & \hat{h}_{eff} \end{pmatrix}, \hat{h}_{eff} = \begin{pmatrix} \epsilon - i\gamma_1 & -u - i\sqrt{\gamma_1\gamma_2} \\ -u - i\sqrt{\gamma_1\gamma_2} & -\epsilon - i\gamma_2 \end{pmatrix}, \quad (5)$$

where according to Tables 2 and 3 In Appendix

$$\epsilon = |k_2|(g(a)^2 - h(a)^2), u = 2|k_2|g(a)h(a), \gamma_1 = \frac{4k_1}{a^2}, \gamma_2 = \frac{2k_1}{\pi^2} \sin^2\left(\frac{2\pi}{a}\right), \quad (6)$$

and according to Eq. (4) in Appendix $k_1 = \nu = \nu_{16} = 5/a, |k_2| = 7/a$.

One can see that the effective Hamiltonian consists of two identical blocks 2×2 , each of them has typical form for description of FW BICs [4, 11, 20]. Comparison with expressions (1) and (3) shows that the eigenmodes (1, 6) and (5, 4) and, respectively, (6, 1) and (4, 5) are coupled through the continuum of waveguides that gives rise to FW mechanism of two degenerate BICs classified according to the two-dimensional irreducible representation E . If we neglected by closed channel, $p = 2$ one could have two degenerate FW BICs for $a > 5$. However, the evanescent modes of waveguides play the principal role because they give rise to real coupling u between modes. For $u \neq 0$, the FW BIC occurs in the framework of the Hamiltonian (5) according to the following equation [4, 20, 37]

$$u(\gamma_1 - \gamma_2) = 2\epsilon\sqrt{\gamma_1\gamma_2}. \quad (7)$$

It is easy to fulfill Eq. (7) if the parameters $u, \gamma_1, \gamma_2, \epsilon$ were independent. However, for the present case all constants depend on only the square size a as given in Eq. (6). As Comsol MultiPhysics shows in Fig. 2 (a) the condition (7) is not fulfilled for variation a that defines the solution as quasi FW BIC although with extremely large Q -factor around 600000. In view material losses of 3d printed acoustic resonators which restrict the Q factor by order of 10^3 [19] one can consider the solution in Fig. 2 (b) as the FW BIC. Remarkably, compared to usual FW BICs with sharp peak in the Q -factor for variation of the sizes of resonator the degenerate FW BICs maintain extremely high Q -factor in wide range of the size. That relieves experimentalists from the fabrication difficulties of proper choice of the resonators.

Fig. 2 (c) clearly shows that this BIC is composed of eigenmodes (1, 6) and (5, 4). The FW BIC composed of the eigenmodes (6, 1) and (4, 5) differs from this solution by 90° rotation.

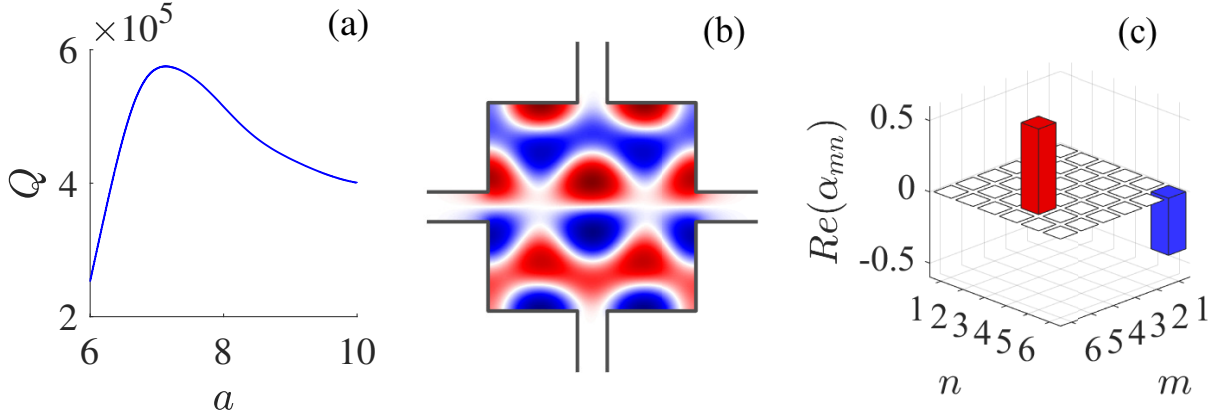


Figure 2. (a) The Q -factor of quasi FW BIC shown in subplot (b) with the modal expansion coefficients shown in (c).

In order to restore true degenerate FW BICs, we attach waveguides at the vertices of the square as shown in Fig. 1 (c) which also give equal couplings of eigenmodes of the square resonator with the continua of waveguides. However similar to side coupling of square with waveguides the evanescent modes remove the number degeneracy of modes 1, 6 and 5, 4. Numerics reveals two degenerate FW BICs with the frequency $\nu = 0.832051$ occur for variation of square size $a = 6.8818$, the first of which is shown in Fig. 3. One can see that FW BIC is superposed of two eigenmodes (1, 6) and (5, 4). The second degenerate FW BIC is obtained by 90° rotation and both BICs are classified according to the two-dimensional representation E .

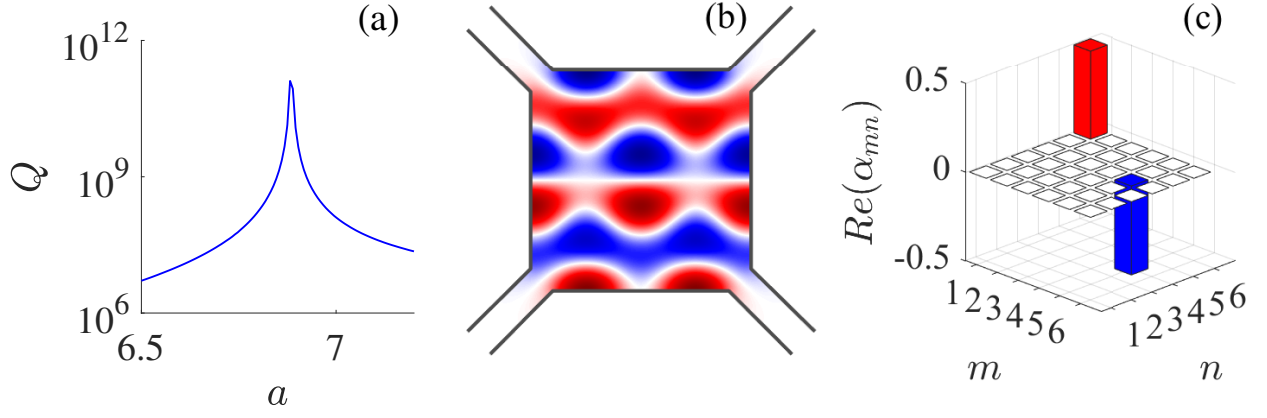


Figure 3. The same as in Fig. 2 but for vertex connection of resonator to waveguides as shown in Fig. 1 (c).

IV. DEGENERATE BICS IN EQUILATERAL TRIANGLE

Less obvious cases of the number degeneracy exist in the equilateral triangle with the eigenmodes and eigenfrequencies presented in Appendix. Similar to a square resonator, all eigenmodes are two-fold degenerate relative to $m \leftrightarrow n$, giving rise to the FW BICs. However there are also exceptional cases of the four-fold accidental number degeneracy, for example, for $m = -11, n = -19$ and $m = -16, n = -17$. Pressure profiles of these four eigenmodes with the lowest frequency $\nu \approx 40$ are shown in Appendix. Respectively, with opening of the triangular resonator with three attached waveguides these four eigenmodes are transformed into two superradiant modes and two FW BICs classified according to the two-dimensional irreducible representation E of group symmetry C_{3v} . Similar to open square resonator, only vertex attachment of waveguides allows existence of degenerate BICs, as shown in Fig. 4. The

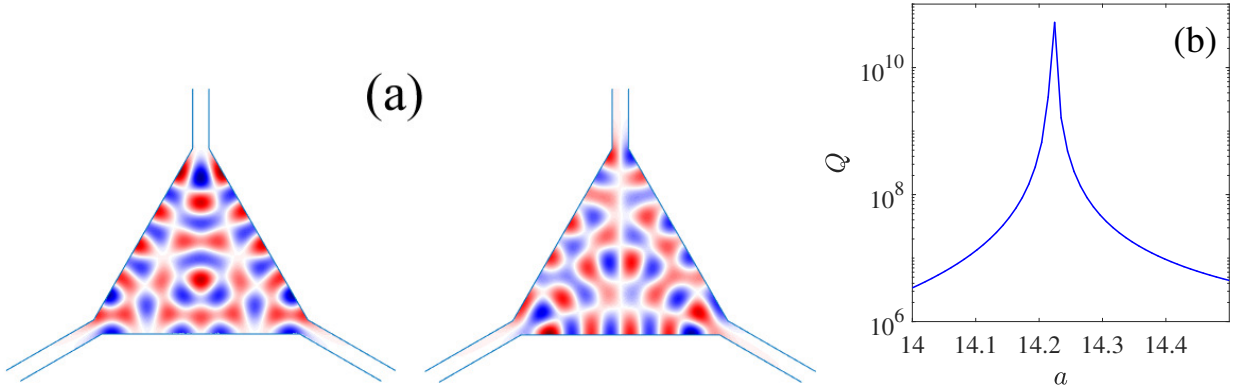


Figure 4. (a) Degenerate BICs with the frequency $\nu_{BIC} = 0.8938$ classified according to the two-dimensional irreducible representation E of group symmetry C_{3v} . $a = a_c = 14.1939$. (b) The Q -factor dependence on side size of triangle a .

resonant eigenmodes of the open triangular resonator can be found only numerically as distinctive from the case of the square open resonator.

The existence of degenerate resonances and, in particular, BICs opens a way of highly effective manipulating out power flows by small perturbations. In particular, that can be done by slight violation of symmetry of the system, say, by slight local pressure onto the resonator walls. In the present letter, we apply a local perturbation in the form of pencil of triangular or rectangular cross-sections at the center of the resonator which can be rotated by the angle θ relative to the resonator. Fig. 5 demonstrates the striking result of the symmetry incompatibility of the resonator and perturbation. Fig. 5 (a) shows that perturbation which preserves the symmetry C_3 of the total system can not manipulate by acoustic flows irrespective of the angle θ . While the perturbation of the symmetry C_2 whose symmetry is not compatible with the symmetry of the total system drastically changes the output acoustic flows.

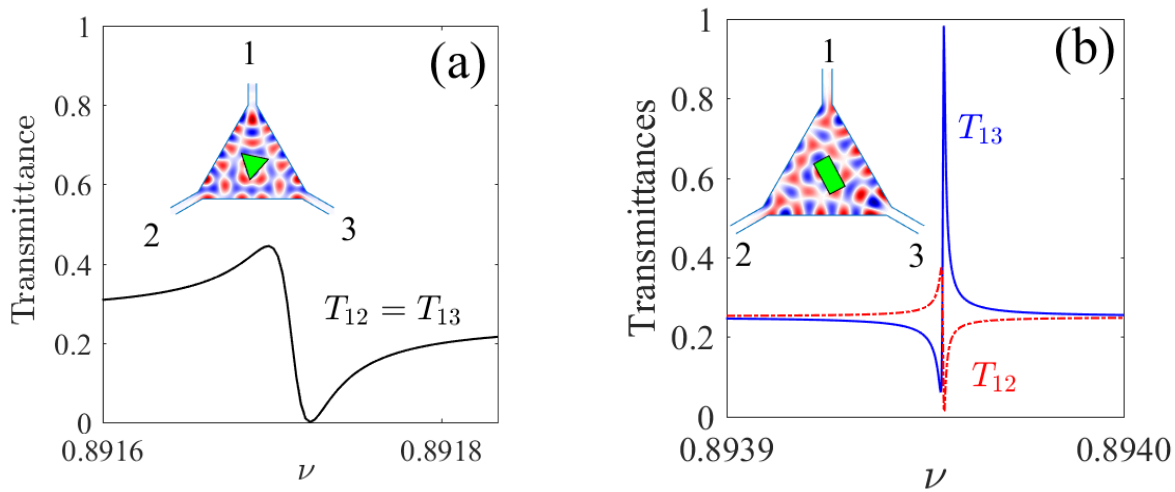


Figure 5. Transmittance from input waveguide 1 into the output waveguides 2 and 3 in the triangular resonator with rotated (a) triangular pencil and (b) rectangular pencil. The frequency of input wave is tuned onto the frequency of degenerate FW BICs shown in Fig. 4.

V. CONCLUSIONS

We considered square and triangular resonators with the symmetries whose eigenmodes are classified to the irreducible representations of group symmetries C_{4v} and C_{3v} among of which there is the two-dimensional representation E . One can preserve the symmetries of open resonators owing to proper connection of waveguides to the resonator as sketched in Fig. 1. The Hamiltonian of closed resonator H_B transforms into non-Hermitian effective Hamiltonian H_{eff} after the Feshbach projection of the total system into space of eigenfunction of H_B [31]. Respectively, the eigenmodes of H_B with real eigenvalues are substituted by resonant modes, which are the eigenmodes of H_{eff} with complex eigenvalues. Both Hamiltonians commute with the symmetry group transformations, and therefore one can expect that there are two-fold degenerate resonant states classified according to the two-dimensional irreducible representation E . However, analytical consideration in Section 3 explicitly shows these resonant states can not be true FW BICs because of the absence of interaction through the continuum of waveguides. In order to realize the degenerate FW BICs, we explore the unique property of square and triangular resonators of numeric accidental degeneracy of eigenmodes. As a result, we obtain the four-fold degeneracy of eigenmodes of H_B which transform into the two-fold degenerate FW BICs and two superradiant resonances. Shaw has presented even more unique cases of number eight-fold degeneracy for $m = 5, n = 34$; $m = 10, n = 33$; $m = 13, n = 32$; $m = 24, n = 25$ with higher eigenfrequencies [22]. Respectively, we can expect the four-fold degenerate FW BICs or go above the first cutoff $\nu = 1$ towards the FW BICs embedded into a few continua of the next propagating bands of waveguides [38]. In general, degenerate BICs can also occur in open systems symmetrical, for example, relative to axial rotations. Then the Hilbert space of total system splits into a direct sum of spaces specified by the azimuthal index m . Respectively, the BICs, if they exist, are degenerate relative to $\pm m$ because of time-reversal symmetry. Examples of such degenerate BICs were reported in the periodical array of dielectric spheres [39] and disks [40]. However, these BICs are not degenerate in each Hilbert subspace specified by the azimuthal index m .

VI. APPENDIX

A. The eigenmodes of square resonator classified according to irreducible representations of square symmetry group C_{4v}

In the acoustic square resonator with the Neumann boundary conditions result in the following eigenmodes

$$\psi_{m,n}(x, y) = \sqrt{\frac{(2 - \delta_{m,1})(2 - \delta_{n,1})}{a}} \cos\left(\frac{\pi(m-1)x}{a}\right) \cos\left(\frac{\pi(n-1)y}{a}\right) \quad (8)$$

Table I. The characters of irreducible representations of group symmetry C_{4v}

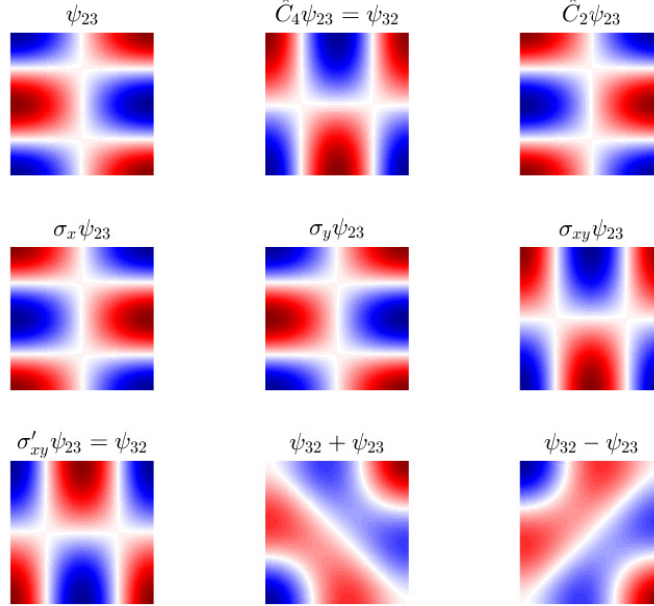
C_{4v}	1	C_2	$2C_4$	σ_x, σ_y	$\sigma_{xy}, \sigma'_{xy}$	basic modes
A_1	1	1	1	1	1	z
A_2	1	1	1	-1	-1	J_z
B_1	1	1	-1	1	-1	$x^2 - y^2$
B_2	1	1	-1	-1	1	xy
E	2	-2	0	0	0	x, y

with the eigenfrequencies

$$\nu_{m,n}^2 = \omega_{m,n}^2 / \omega_0^2 = (m-1)^2 + (n-1)^2, m, n = 1, 2, 3, \dots, \quad (9)$$

where $\omega_0 = \pi s/a$, s is the velocity of sound in air and a is the size of square.

The group of symmetry C_{4v} of square consists of rotations C_4 and C_2 , two mirror reflections σ_v along the square axis x and y and σ'_v along the diagonals of square [41, 42]. Tabl. I shows the irreducible representations of each symmetry transformation and their characters [42]. Fig. 6 shows that the eigenmodes $\psi_{m,2n+1}$ and $\psi_{2n+1,m}$ belong to the two-dimensional irreducible representation E . However the eigenmodes $\psi_{2m,2m+2n}$ and $\psi_{2m+2n,2m}$ are classified by the reducible representations. As Fig. 7 shows only the linear combinations $\psi_{2m+2n,2m} + \psi_{2m,2m+2n}$ and $\psi_{2m+2n,2m} - \psi_{2m,2m+2n}$ are classified according to the irreducible one-dimensional representations B_2 and A_2 respectively. Similarly, the linear combinations $\psi_{2m+2n+2,2m+1} + \psi_{2m+1,2m+2n+2}$ and $\psi_{2m+2n+2,2m+1} - \psi_{2m+1,2m+2n+2}$ are classified according to the irreducible one-dimensional representations B_1 and A_1 respectively. In Fig. 8 we present

Figure 6. Symmetry group C_{4v} transformations of the eigenmode $\psi_{23}(x, y)$.

an example of eigenmodes ψ_{16} and ψ_{54} degenerated accidentally [22, 23].

B. Effective non Hermitian Hamiltonian

The procedure of the Feshbach projection of the total Hilbert space of the total system closed resonator plus waveguides with Neumann boundary conditions onto Hilbert space of the eigenmodes of closed resonator is described

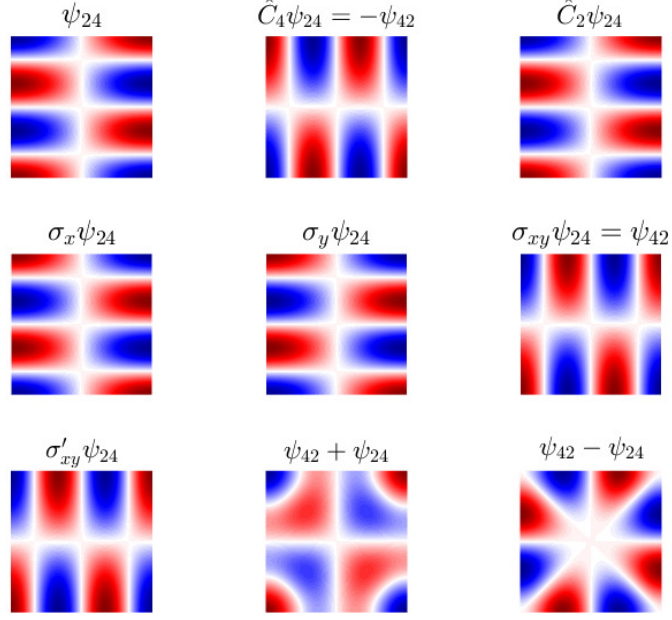


Figure 7. Symmetry group C_{4v} transformations for the eigenmode $\psi_{24}(x, y)$.

in Ref. [36]. In application to the square acoustic resonator we have

$$\hat{H}_{eff} = \nu_{mn}^2 \delta_{mm'} \delta_{nn'} - \sum_{p=1}^{\infty} \sum_C i k_p \hat{W}_{Cp} \hat{W}_{Cp}^\dagger, \quad (10)$$

where k_p are the propagating momenta of the p -th channel in waveguides of width d . In what follows all dimensions are measured in terms of d , i.e., $d = 1$. Then

$$\nu^2 = k_p^2 + (p-1)^2, p = 1, 2, 3, \dots \quad (11)$$

with

$$\phi_p(x, y) = \sqrt{2 - \delta_{p,1}} \cos(\pi(p-1)y) e^{ik_p x}. \quad (12)$$

The index w in Eq. (10) sorts waveguides. For attachments of waveguides shown in Fig. 1 of the main text the coupling matrix \hat{W}_{Cp} can be evaluated analytically

$$W_{mn;p,C=1,3} = \int_{-1/2}^{1/2} \psi_{mn}(x = \mp a/2, y) \phi_p(y) dy, \quad (13)$$

$$W_{mn;p,C=2,4} = \int_{-1/2}^{1/2} \psi_{mn}(x, y = \pm a/2) \phi_p(x) dx. \quad (14)$$

After integration in geometry shown in Fig. 1 (b) of the paper we obtain for the waveguide 1:

$$W_{mn;p,C=1} = \frac{\sqrt{(2-\delta_{m,1})(2-\delta_{n,1})(2-\delta_{p,1})}}{\pi} \left\{ \frac{\sin[\frac{\pi}{2a}(n-1+a(p-1))] \cos[\frac{\pi}{2}(n-1+a(p-1))]}{n-1+a(p-1)} + \frac{\sin[\frac{\pi}{2a}(n-1-a(p-1))] \cos[\frac{\pi}{2}(n-1-a(p-1))]}{n-1-a(p-1)} \right\}. \quad (15)$$

Some particular coupling matrix elements relevant for the paper are collected in Tables II and III where according

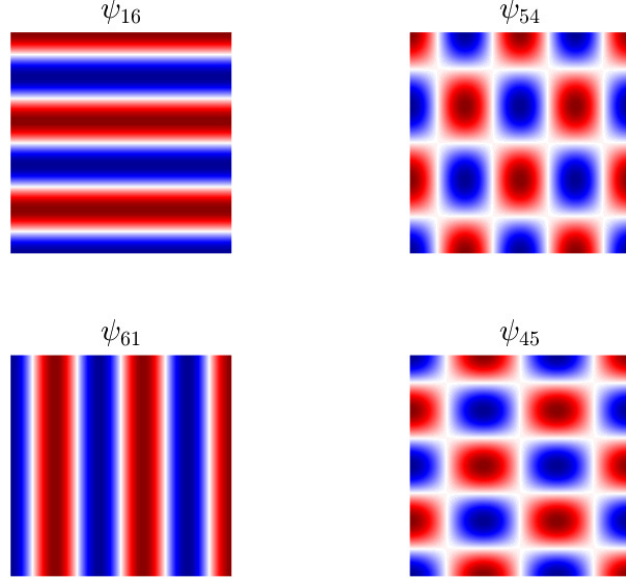


Figure 8. The number degenerated eigenfunctions of square.

Table II. Coupling matrix elements with the first open channel $p = 1$

modes $m, n \setminus C$	1	2	3	4
2, 3	$-\frac{2}{\pi} \sin \frac{\pi}{a}$	0	$\frac{2}{\pi} \sin \frac{\pi}{a}$	0
3, 2	0	$\frac{2}{\pi} \sin \frac{\pi}{a}$	0	$-\frac{2}{\pi} \sin \frac{\pi}{a}$
2, 4	0	0	0	0
4, 2	0	0	0	0
1, 6	0	$\frac{\sqrt{2}}{a}$	0	$-\frac{\sqrt{2}}{a}$
5, 4	0	$\frac{1}{\pi} \sin \frac{2\pi}{a}$	0	$-\frac{1}{\pi} \sin \frac{2\pi}{a}$
6, 1	$\frac{\sqrt{2}}{a}$	0	$-\frac{\sqrt{2}}{a}$	0
4, 5	$\frac{1}{\pi} \sin \frac{2\pi}{a}$	0	$-\frac{1}{\pi} \sin \frac{2\pi}{a}$	0

to Eq. (15) we denote

$$\begin{aligned}
 b(a) &= \frac{4\sqrt{2}a}{\pi(a^2-9)} \sin \frac{\pi a}{2} \cos \frac{3\pi}{2a}, \\
 c(a) &= \frac{4\sqrt{2}a}{\pi(a^2-4)} \sin \frac{\pi a}{2} \cos \frac{\pi}{2a}, \\
 f(a) &= \frac{4\sqrt{2}a}{\pi(a^2-4)} \cos \frac{\pi}{a} \cos \frac{\pi a}{2}, \\
 g(a) &= -\frac{4a}{\pi(a^2-25)} \cos \frac{5\pi}{2a} \sin \frac{\pi a}{2}, \\
 h(a) &= \frac{4\sqrt{2}a}{\pi(a^2-16)} \cos \frac{2\pi}{a} \cos \frac{\pi a}{2}.
 \end{aligned} \tag{16}$$

C. Eigenmodes of equilateral triangular billiard

The eigenfrequencies of equilateral triangle equal for the Neumann boundary conditions

$$\nu_{mn}^2 = \omega_{mn}^2 / \omega_0^2 = \frac{16}{27}(m^2 + n^2 - mn), m, n = 0, \pm 1, \pm 2, \dots, \tag{17}$$

Table III. Coupling matrix elements with the second closed channel $p = 2$

modes $m, n \setminus C$	1	2	3	4
2, 3	0	$-f(a)$	0	$f(a)$
3, 2	$-f(a)$	0	$f(a)$	0
2, 4	$-b(a)$	$-c(a)$	$b(a)$	$c(a)$
4, 2	$c(a)$	$b(a)$	$-c(a)$	$-b(a)$
1, 6	$g(a)$	0	$g(a)$	0
5, 4	$-h(a)$	0	$-h(a)$	0
6, 1	0	$g(a)$	0	$g(a)$
4, 5	0	$h(a)$	0	$h(a)$

where ω_0 is defined in Eq. (9) with the following conditions: $m + n$ is a multiple of 3 [43]. The eigenmodes are of the form

$$\begin{aligned}\psi_{mn} &= f_{mn} + f_{m,m-n} + f_{-n,m-n} + f_{-n,-m} + f_{n-m,-m} + f_{n-m,n} \\ f_{mn}(x, y) &= \exp(2\pi i/3)(nx + (2n - m)y/\sqrt{3}).\end{aligned}\quad (18)$$

In Fig. 9 we show patterns of the eigenmodes which are four fold degenerate due to permutation symmetry $m \leftrightarrow n$ and accidental number degeneracy at $m = -16, n = -17$ and $m = 11, n = -19$.

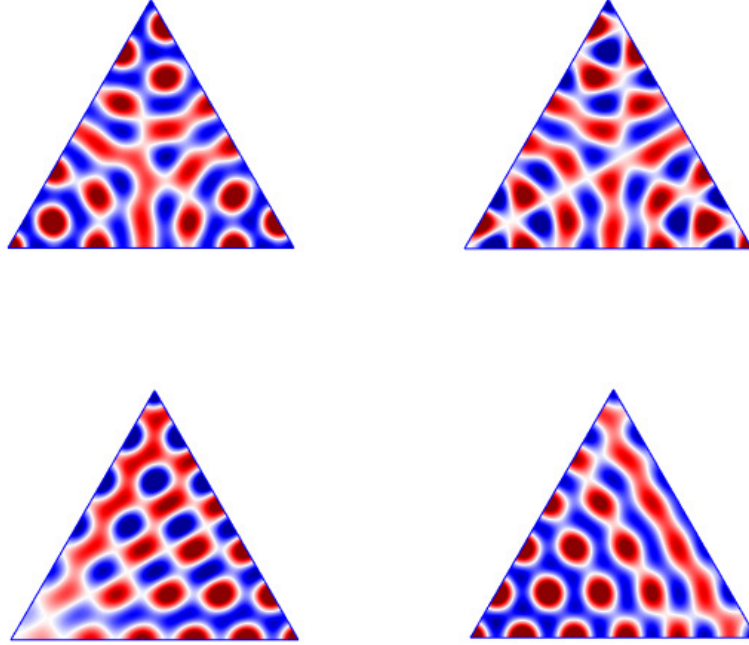


Figure 9. Four fold degenerate eigenvalues of equilateral triangle with eigenfrequencies $\nu_{-11,-19}^2 = \nu_{-16,-17}^2 = 161.778$.

There are also other cases of the four fold degeneracy however with higher eigenfrequencies with $m = -13, n = -23, m = -23, n = -13$ and $m = -17, n = -22, m = -22, n = -17$ with the eigenvalue $\nu_{-13,-23}^2 = 226.312$. The group of symmetry C_{3v} of equilateral triangle consists of rotations C_3 , mirror reflections σ_v along the diagonals of resonator [42]. Tabl. IV shows the irreducible representations of each symmetry transformation and their characters [42].

Table IV. The characters of irreducible representations of group symmetry C_{3v}

C_{3v}	1	$2C_3$	$3\sigma_v$	basic modes
A_1	1	1	1	z
A_2	1	1	-1	J_z
E	2	-1	0	x, y

-
- [1] Chia Wei Hsu, Bo Zhen, A. D. Stone, J. D. Joannopoulos, and M. Soljačić, Bound states in the continuum, *Nature Reviews Materials* **1**, 16048 (2016).
- [2] G. Quaranta, G. Basset, O. J. F. Martin, and B. Gallinet, Recent advances in resonant waveguide gratings, *Laser & Photonics Reviews* **12**, 1800017 (2018).
- [3] L. Huang, L. Xu, M. Woolley, and A. E. Miroshnichenko, Trends in quantum nanophotonics, *Advanced Quantum Technologies* **3**, 1900126 (2020).
- [4] A. F. Sadreev, Interference traps waves in an open system: bound states in the continuum, *Reports on Progress in Physics* **84**, 055901 (2021).
- [5] S. Joseph, S. Pandey, S. Sarkar, and J. Joseph, Bound states in the continuum in resonant nanostructures: an overview of engineered materials for tailored applications, *Nanophotonics* **10**, 4175 (2021).
- [6] M. Bolsterli, Continuity of phase shift at continuum bound state, *Phys. Rev.* **182**, 1095 (1969).
- [7] M. Robnik, A simple separable Hamiltonian having bound states in the continuum, *J. Phys. A: Math. Gen.* **19**, 3845 (1986).
- [8] R. L. Schult, D. G. Ravenhall, and H. W. Wyld, Quantum bound states in a classically unbound system of crossed wires, *Phys. Rev. B* **39**, 5476 (1989).
- [9] D. Evans and R. Porter, Trapped modes embedded in the continuous spectrum, *The Quarterly Journal of Mechanics and Applied Mathematics* **51**, 263 (1998).
- [10] N. Moiseyev, Suppression of Feshbach resonance widths in two-dimensional waveguides and quantum dots: A lower bound for the number of bound states in the continuum, *Phys. Rev. Lett.* **102**, 167404 (2009).
- [11] H. Friedrich and D. Wintgen, Interfering resonances and bound states in the continuum, *Phys. Rev. A* **32**, 3231 (1985).
- [12] A. F. Sadreev, E. N. Bulgakov, and I. Rotter, Bound states in the continuum in open quantum billiards with a variable shape, *Phys. Rev. B* **73**, 235342 (2006).
- [13] C. Linton, M. McIver, P. McIver, K. Ratcliffe, and J. Zhang, Trapped modes for off-centre structures in guides, *Wave Motion* **36**, 67 (2002).
- [14] Y. Duan, W. Koch, C. Linton, and M. McIver, Complex resonances and trapped modes in ducted domains, *J. Fluid Mech.* **571**, 119 (2007).
- [15] S. Hein and W. Koch, Acoustic resonances and trapped modes in pipes and tunnels, *J. Fluid Mech.* **605**, 401 (2008).
- [16] A. A. Lyapina, D. N. Maksimov, A. S. Pilipchuk, and A. F. Sadreev, Bound states in the continuum in open acoustic resonators, *J. Fluid Mech.* **780**, 370 (2015).
- [17] S. Huang, T. Liu, Z. Zhou, X. Wang, J. Zhu, and Y. Li, Extreme sound confinement from quasibound states in the continuum, *Phys. Rev. Applied* **14**, 021001 (2020).
- [18] T. Lepetit and B. Kanté, Controlling multipolar radiation with symmetries for electromagnetic bound states in the continuum, *Phys. Rev. B* **90**, 241103(R) (2014).
- [19] L. Huang, Y. K. Chiang, S. Huang, C. Shen, F. Deng, Y. Cheng, B. Jia, Y. Li, D. A. Powell, and A. E. Miroshnichenko, Sound trapping in an open resonator, *Nature Communications* **12**, 4819 (2021).
- [20] A. Volya and V. Zelevinsky, Non-hermitian effective Hamiltonian and continuum shell model, *Phys. Rev. C* **67**, 054322 (2003).
- [21] A. Lyapina, A. Pilipchuk, and A. Sadreev, Trapped modes in a non-axisymmetric cylindrical waveguide, *J. Sound and Vibr.* **421**, 48 (2018).
- [22] G. B. Shaw, Degeneracy in the particle in a box problem, *J. Phys. A: Math., Nuclear and Gen.* **7**, 1537 (1974).
- [23] J. R. Kuttler and V. G. Sigillito, Eigenvalues of the laplacian in two dimensions, *SIAM Review* **26**, 163 (1984).
- [24] S. Gladyshev, K. Frizyuk, and A. Bogdanov, Symmetry analysis and multipole classification of eigenmodes in electromagnetic resonators for engineering their optical properties, *Phys. Rev. B* **102**, 075103 (2020).
- [25] L. Huang, L. Xu, M. Rahmani, D. Neshev, and A. Miroshnichenko, Pushing the limit of high-Q mode of a single dielectric nanocavity, *Adv. Photonics* **3**, 016004 (2021).
- [26] K. Pichugin, A. Sadreev, and E. Bulgakov, Ultrahigh-Q system of a few coaxial disks, *Nanophotonics* **10**, 4314 (2021).
- [27] A. Overvig, S. Malek, M. Carter, S. Shrestha, and N. Yu, Selection rules for quasibound states in the continuum, *Phys. Rev. B* **102**, 035434 (2020).
- [28] A. Overvig, N. Yu, and A. Alù, Chiral quasi-bound states in the continuum, *Phys. Rev. Lett.* **126**, 073001 (2021).
- [29] V. Dmitriev, A. Kupriianov, S.D.S.S., and V. Tuz, Symmetry analysis of trimer-based all-dielectric metasurfaces with toroidal dipole modes, *J. Phys. D: Appl. Phys.* **54**, 115107 (2021).

- [30] M. Tsimokha, V. Igoshin, A. Nikitina, M. Petrov, I. Toftul, and K. Frizyuk, Acoustic resonators: symmetry classification and multipolar content of the eigenmodes, *ArXiv: 2110.11220v1* (2021).
- [31] H. Feshbach, Unified theory of nuclear reactions, *Ann. Phys.* **5**, 357 (1958).
- [32] H. Feshbach, A unified theory of nuclear reactions. II, *Ann. Phys.* **19**, 287 (1962).
- [33] I. Rotter, A continuum shell model for the open quantum mechanical nuclear system, *Reports on Progress in Physics* **54**, 635 (1991).
- [34] F. Dittes, The decay of quantum systems with a small number of open channels, *Physics Reports* **339**, 215 (2000).
- [35] A. Sadreev and I. Rotter, S-matrix theory for transmission through billiards in tight-binding approach, *Journal of Physics A: Math. Gen.* **36**, 11413 (2003).
- [36] D. N. Maksimov, A. F. Sadreev, A. A. Lyapina, and A. S. Pilipchuk, Coupled mode theory for acoustic resonators, *Wave Motion* **56**, 52 (2015).
- [37] R. Kikkawa, M. Nishida, and Y. Kadoya, Polarization-based branch selection of bound states in the continuum in dielectric waveguide modes anti-crossed by a metal grating, *New Journal of Physics* **21**, 113020 (2019).
- [38] F. Remacle, M. Munster, V. Pavlov-Verevkin, and M. Desouter-Lecomte, Trapping in competitive decay of degenerate states, *Phys. Lett. A* **145**, 265 (1990).
- [39] E. N. Bulgakov and A. F. Sadreev, Light trapping above the light cone in a one-dimensional array of dielectric spheres, *Phys. Rev. A* **92**, 023816 (2015).
- [40] E. N. Bulgakov and A. F. Sadreev, Bound states in the continuum with high orbital angular momentum in a dielectric rod with periodically modulated permittivity, *Phys. Rev. A* **96**, 013841 (2017).
- [41] L. D. Landau and E. M. Lifshitz, *Quantum Mechanics: Non-relativistic Theory. V. 3 of Course of Theoretical Physics* (Pergamon Press, 1958).
- [42] G. L. Bir and G. E. Pikus, *Symmetry and strain-induced effects in semiconductors* (Wiley New York, 1974).
- [43] M. A. Pinsky, The eigenvalues of an equilateral triangle, *SIAM J. Math. Analysis* **11**, 819 (1980).